

Effects of Denaturation on the Structure and Properties of Soy Protein Composites

Allen Eyler¹, Tian Liu¹, Louis Scudiero², Pui Ching Wo³ and Wei-Hong Zhong^{1,*}

¹*School of Mechanical and Materials Engineering, Composite Materials and Engineering Center, Washington State University, U.S*

²*Department of Chemistry, Washington State University, U.S*

³*School of Mechanical and Materials Engineering, Washington State University, U.S*

Abstract: Soy protein (SP), a widely abundant biomaterial with a high concentration of polar and reactive functional groups and a complex three dimensional structure, has frequently been used in polymer blends and composites. However, few studies have focused on the critical role of denaturation in the application of SP to composites. The denaturation conditions profoundly affect the protein structure at scales approaching the molecular level and therefore can be expected to significantly influence the morphology and properties of SP-containing composites. In this study, the influences of three SP denaturation methods on the structures and properties of the poly(ethylene oxide) (PEO) composite films were compared. Of these methods, urea treatment followed by dialysis process results in the most effective denaturation, with nanoscale SP particle size and high PEO/SP interfacial area, stable dielectric properties, and super-elasticity resulting from improved PEO/SP interactions. This work guides the customization of biocomposite properties *via* the control of denaturation conditions.

Keywords: Biopolymers, biocomposites, denaturation, thermal properties, mechanical properties, dielectric properties.

1. INTRODUCTION

Soy protein (SP) has drawn much attention in materials research due to its wide abundance and renewability, ability to form films, gas barrier properties, as well as high modulus of elasticity. It has mainly been used in polymer blends and composites for food packaging [1], biomedical, and antimicrobial [2] applications. One of the most intriguing aspects of the widely used SP is its variety of functional groups, which give rise to many types of intermolecular interactions. In the protein's native state, however, most of these functional groups are trapped within the globular structure and are unavailable for interaction with other components [3]. Therefore, the process of denaturation is critical to the effective use of SP in biocomposite materials.

As a protein material, SP possesses highly complex chemical and physical structures. The molecules that make up SP are composed of 21 different amino acids, 39% of which are non-polar, and around 58% of which are polar [4, 5]. This results in a complex set of intra- and intermolecular interactions, including ionic, van der Waals, and covalent bonding, which in turn creates an intricate structure with four levels. The primary structure refers to the sequence of amino acids which form the polypeptide chain; secondary structure refers

to short-range order, such as α -helices and β -sheets; the tertiary structure describes the overall three-dimensional folding of the molecule; and the quaternary structure is the bonding of separate chains (subunits) to form larger structures. During the process of denaturation, many of the intermolecular bonds can be broken resulting in reconfigured secondary, tertiary, and quaternary structures. This results in many of the previously buried functional groups becoming exposed and available to interact with other components.

A wide variety of techniques have been applied for the SP denaturation [6]. One of the simplest and most common denaturation methods is thermal denaturation; the main SP fractions, 7S and 11S, are denatured at 77.1 and 93.3°C, respectively [7]. Another common way is to adjust the pH to values above or below the protein's isoelectric point of approximately 4.5, which results in electrostatic repulsion of the protein chains as acidic and basic functional groups become charged [8]. Additionally, denaturation can be aided by the addition of organic solvents to aqueous solution, which disrupt the hydrogen bonds that form the secondary structure [9]. Urea, as a hydrogen bond acceptor, is widely used for the denaturation of proteins [10], including SP [11]. Other denaturation agents for SP including sodium dodecyl sulfate [12], a surfactant that interacts with the hydrophobic groups of the protein, and 2-mercaptoethanol [13], a reducing agent that breaks disulfide linkages between molecules, have been also applied.

*Address correspondence to this author at the School of Mechanical and Materials Engineering, Washington State University, P.O. BOX 642920, Pullman, WA 99164-2920; Tel: 1 509 335 7658; E-mail: katie_zhong@wsu.edu

Despite the extensive studies on the denaturation of SP, and the wide use of SP in composite materials, there have been very few studies on the comparison of these SP denaturation methods, and the relationship between the specific denaturation condition and the structures and properties of the resulting composites. In this work, we compared the effects of different denaturation conditions on the morphologies and properties of composite films consisting of soy protein isolate (SPI), a product consisting of over 90% protein, and PEO. Three different denaturation conditions were applied: thermal denaturation, use of a mixture of acetic acid and water, and dialysis process using urea. The influence of the denatured state of SPI on the morphology, thermal behaviors, dielectric and mechanical properties were investigated.

2. EXPERIMENTAL

2.1. Materials

Poly(ethylene oxide) ($M_v \sim 4,000,000$) and dialysis sacks (average flat width 25mm, MWCO 12 kDa) were obtained from Sigma-Aldrich Co. Soy protein isolate was generously donated by Archer Daniels Midland Co. Sodium Hydroxide ($\geq 98.9\%$) and acetic acid (glacial) were purchased from J.T. Baker.

2.2. Sample Preparation

Samples were prepared by solution casting. Three preparation methods, each with a different denaturation technique, were used. These methods include thermal denaturation, denaturation of the protein *via* urea followed by dialysis, and denaturation in aqueous acetic acid solution.

Thermal denaturation: SPI powder was added to deionized water at a concentration of 1%. To denature the protein, the solution was heated at 90-100°C in an oil bath for 1 hour while stirring continuously. After cooling to room temperature, this solution was blended with a pre-prepared solution of 1% PEO in deionized water, with SPI:PEO mass ratios of 1:9, 1:3, 1:1, and 2:1. PEO/SPI solutions were spin mixed until homogeneous (10 minutes), and then cast onto aluminum foil (for dielectric testing) and polyethylene substrates, and allowed to dry at room temperature.

Dialysis treatment: SPI powder was added to 26.5% urea solution at pH 11, such that the overall SPI concentration was 1%. To denature the protein, the solution was heated at 90-100°C in an oil bath for 1 hour while stirring continuously. Roughly 40mL of the

denatured solution was placed inside a dialysis membrane, which was sealed at both ends. To remove the urea from the solution, the membrane was placed in a 4-liter reservoir of water at pH 11, with gentle magnetic stirring. After 4 hours, the buffer was replaced with a fresh buffer, also at pH 11. After an additional 4 hours of dialysis, the protein solution was removed from the membrane and blended with a pre-prepared solution of 1% PEO in water at pH 11, with SPI:PEO mass ratios of 1:9, 1:3, 1:1, and 2:1. PEO/SPI solutions were spin mixed until homogeneous (10 minutes), and then cast onto aluminum foil (for dielectric testing) and polyethylene substrates, and allowed to dry at room temperature.

Acetic acid treatment: SPI powder was added to a mixed solvent consisting of acetic acid and water in a 4:1 mass ratio, such that the overall SPI concentration was 1%. To denature the protein, the solution was heated at 90-100°C in an oil bath for 1 hour while stirring continuously. After cooling to room temperature, this solution was blended with a pre-prepared solution of 1% PEO in the same solvent, with SPI:PEO mass ratios of 1:9, 1:3, 1:1, and 2:1. PEO/SPI solutions were spin mixed until homogenous (10 minutes), and then cast onto aluminum foil (for dielectric testing) and polyethylene substrates, and allowed to dry at room temperature.

2.3. Characterizations

SEM Imaging and Particle Size Measurements: Samples were fractured under liquid nitrogen to avoid plastic deformation, and the fracture surfaces were observed by a FEI Quanta 200F scanning electron microscope. For particle size measurements, 25-50 particles were measured for each sample by drawing a line across the longest axis of each particle in Image J, an image-analysis software tool, and measuring the length of the lines.

To characterize the crystalline morphology of the samples, optical images were collected *via* a Leica LM750 microscope. Sections of each film were pressed between two glass slides, and images were taken at a magnification of 10X with a polarizing filter applied.

Differential scanning calorimetry (DSC) was performed using a TA DSC 2920 Modulated DSC to study the thermal behaviors of the PEO/SPI films. In the DSC procedure, samples were first heated from room temperature to 120°C at a rate of 10°C per minute. Melting enthalpy was calculated from the heating curve and was normalized to the concentration

of PEO in the sample. Sample masses were approximately 8mg.

Alternating current (AC) conductivity was obtained at ambient conditions using a Novocontrol Technologies Alpha-N high resolution Dielectric Analyzer. Prior to testing, samples were heated at 50°C in a vacuum oven for 24 hours to remove residual solvent.

Nanoindentation was performed using a Hysitron TI 900 TriboIndenter in nanoDMA mode. The static load started at 50.00 μ N and increased linearly to 200.00 μ N at a rate of 10.00 μ N/s. The dynamic load had an amplitude of 1.00 μ N with a frequency of 30.00 Hz. Four indentations were performed on each sample, and the average hardness was determined for each sample.

3. RESULTS AND DISCUSSION

3.1. Composite Morphology and Particle Size

To compare the morphologies of the composite samples with different SPI concentrations and denaturation conditions, fracture surfaces of the com-

posites were imaged *via* SEM, as shown in Figure 1. From the images, SPI particles could be measured and the distribution of particle sizes could be obtained; particle size distributions are shown in Figure 2. Comparing the SPI particle size for the samples with the same SPI concentration, there are clear differences in the composites with different denaturation conditions. At 10% SPI concentration, the sample with dialysis-treated SPI shows the smallest particle size, with a modal particle diameter of roughly 20nm; SPI denatured in the mixed acetic acid/water solvent has a larger modal diameter of around 50nm; and thermally denatured SPI has the largest size of around 200nm. With the increase in SPI content, the particle size increases significantly for all SPI denaturation conditions. This phenomenon is more obvious for the samples treated by mixed solvent and thermal denaturation. As we can observe from Figure 1 (l and d), at 67% SPI concentration, the particle sizes for the mixed solvent treated and thermally denatured SPI increased to 200nm and 600nm, respectively. This result is expected; as the number of SPI molecules in a given volume of solution increases, there is a greater probability of intermolecular interaction, resulting in the

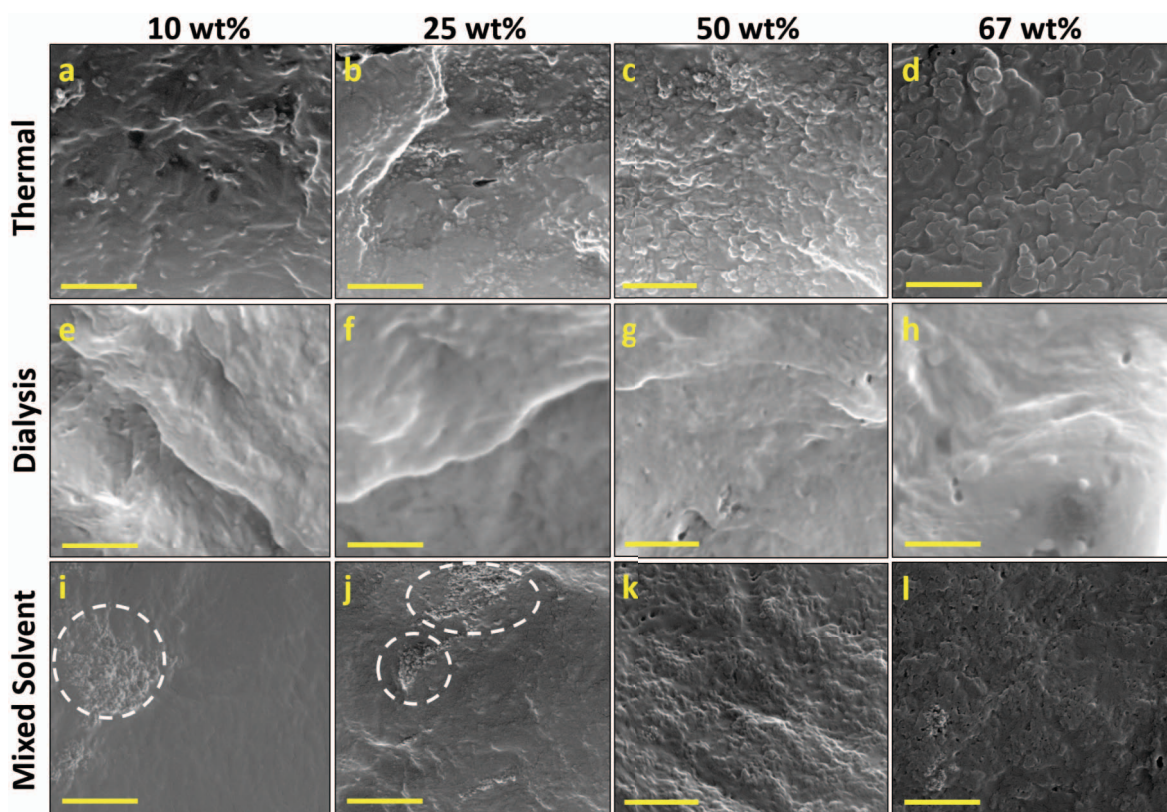


Figure 1: SEM images (scale bar: 1 μ m) showing the morphologies of PEO/SPI blends with varying SPI denaturation conditions and concentrations. Images (a), (b), (c), and (d) show 10%, 25%, 50%, and 67% thermally denatured SPI, respectively; (e), (f), (g), and (h) show 10%, 25%, 50%, and 67% dialysis-treated SPI, respectively; and (i), (j), (k), and (l) show 10%, 25%, 50%, and 67% mixed solvent treated SPI, respectively. Aggregates of SPI particles can be seen in samples prepared *via* mixed solvent (circled in white).

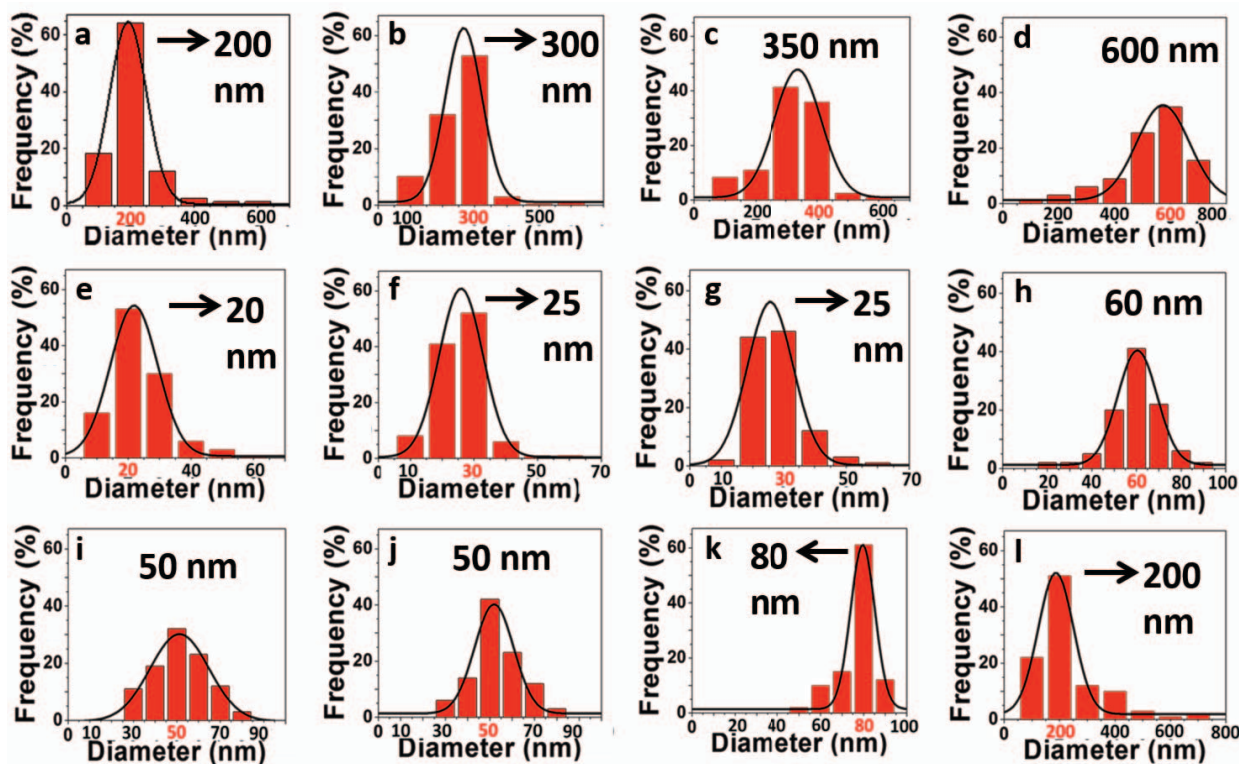


Figure 2: Particle size distributions derived from SEM images. Parts (a), (b), (c), and (d) show 10%, 25%, 50%, and 67% thermally denatured SPI, respectively; (e), (f), (g), and (h) show 10%, 25%, 50%, and 67% dialysis-treated SPI, respectively; and (i), (j), (k), and (l) show 10%, 25%, 50%, and 67% mixed solvent treated SPI, respectively.

formation of larger particles. However, the dialysis method can contribute to the restraint of particle growth with the increase in protein concentration. At 67% SPI loading, a small particle diameter with below 100nm can be maintained, as the peak of the particle size distribution is at 60nm (Figure 2(h)). Therefore, we can draw inferences about the effectiveness of each denaturation condition; when the protein is more effectively denatured, a greater proportion of intermolecular bonds are broken, resulting in a smaller SPI particle size. It appears that the dialysis technique is the most effective denaturation technique, followed

by treatment with acetic acid. This is a logical result since the dialysis technique makes use of urea, a powerful protein-denaturing agent. On the other hand, thermal denaturation in water without the help of additional chemical agents is relatively ineffective, since it is difficult to break the strong hydrophobic interactions within the protein.

3.2. PEO Crystalline Behavior

DSC and optical microscopy were performed in order to characterize the crystalline behaviors of the PEO/SPI blends; results are shown in Table 1 and

Table 1: Melting Enthalpy and T_m for PEO/SPI Films

SPI Denaturation Method	Melting Enthalpy (J/g PEO)				
	0% SPI	10% SPI	25% SPI	50% SPI	67% SPI
Thermal	128.8 ± 8.8	131.6 ± 6.6	133.2 ± 7.4	138.6 ± 3.5	131.2 ± 0.7
Dialysis	131.1 ± 0.1	107.4 ± 14.5	111.9 ± 2.6	112.2 ± 16.8	106.0 ± 8.0
Mixed solvent	126.3 ± 2.9	119.5 ± 1.0	125.9 ± 5.9	115.5 ± 1.6	94.8 ± 3.2
SPI Denaturation Method	T_m (°C)				
	0% SPI	10% SPI	25% SPI	50% SPI	67% SPI
Thermal	73.0 ± 0.7	73.2 ± 2.4	71.2 ± 1.6	67.5 ± 0.0	67.6 ± 0.2
Dialysis	71.9 ± 0.2	70.4 ± 0.2	69.7 ± 0.6	66.8 ± 1.0	66.7 ± 1.3
Mixed solvent	76.3 ± 1.5	70.7 ± 0.3	69.1 ± 0.5	66.1 ± 0.9	63.5 ± 0.7

Figure 3. Inset in Figure 3 are images of laser light scattering by corresponding suspension of SPI solutions, from which information about the particle size in solution, and therefore the denaturation degree, can be inferred. From Table 1, the denatured SPI prepared by three different methods have similar effects on the melting temperature of the composites; T_m tends to decrease with increasing SPI concentration. This indicates that the three SPI denaturation methods had little influence on the thermodynamics of the composites. As presented in Figure 3, the optical micrographs show similar patterns in crystal morphology for dialysis-treated and mixed solvent-treated SPI. At 10% SPI, PEO spherulites can be clearly seen, with a diameter of roughly 200nm. As the SPI concentration is increased to 25%, there is a corresponding increase in the spherulite size. After further increase to 50%, the spherulite boundaries become fainter, and the PEO crystals are invisible or barely visible at 67% SPI. Thermally denatured SPI,

however, shows markedly different effects on the crystalline morphology. At 10% and 25% SPI concentration, the spherulites appear very similar to those of pure PEO; unlike the dialysis-treated and mixed solvent-treated SPI, thermally denatured SPI does not appear to have significant effects on the spherulite size. It is possible that this is due to relatively poor denaturation; strong protein-protein interactions and large particle size limit the ability of this type of SPI to significantly interact with PEO and alter the morphology. As further evidence to support this explanation, the photo of the thermally denatured SPI solution shows that it is almost completely opaque, suggesting very large particles that completely scatter any light that enters the solutions; by contrast, the dialyzed and mixed solvent-treated SPI solutions are translucent, implying that the protein particles are too small to completely scatter visible light.

Comparison of melting enthalpies for the composites in Table 1 shows that the melting enthalpy (and therefore the crystallinity) is relatively constant with increasing SPI concentration for all three types of SPI. Although PEO-SPI interaction is strong enough to affect the PEO crystal morphology when certain denaturation conditions are applied, this interaction is not strong enough to suppress the crystallization of PEO, even at very high SPI concentrations.

3.3. Dielectric Properties

The dielectric properties of the PEO/SPI composites were analyzed in order to gain further insight on the PEO-SPI interactions in these composites with different SPI denaturation methods; results are plotted in Figure 4. As indicated, the dielectric constant was decreased with increasing SPI concentration for all three protein denaturation methods, with around 1 order of magnitude decrease in the composite with dialysis treated SPI, 1.5 orders reduction in thermally denatured protein, and almost 3 orders decrease in the sample with mixed solvent treated SPI at 10^{-2} Hz (Figure 4, first row). This can be described by the Maxwell-Wagner-Sillars interfacial polarization mechanism, in which the interfacial polarization effect can result in the increased dielectric constant of multiphase composite systems [14-15]. Although the SPI concentration increased from 10wt% to 67%, the interfacial areas were not increased simultaneously; instead, the loading of SPI is inversely proportional to the interfacial area between the protein and PEO matrix. This is because of the aggregation of the protein particles at a high concentration, as explained

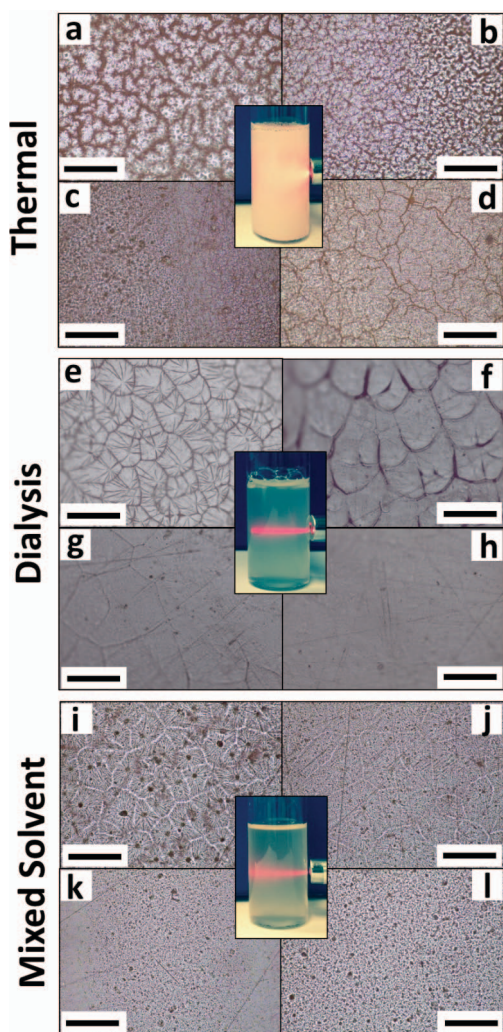


Figure 3: Optical micrographs (scale bar: 100 μ m) showing the crystal morphology of PEO, with insets showing laser light scattering by denatured SPI solutions.

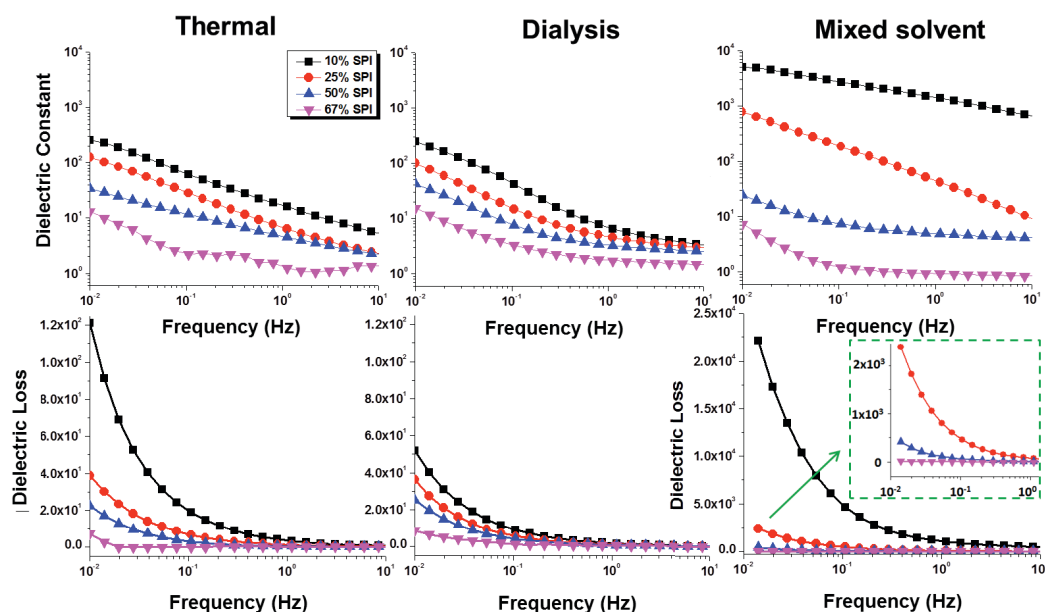


Figure 4: Dependence of dielectric constant (first row) and dielectric loss (second row) on the frequency for the three SPI denaturation conditions.

in the morphology studies (Figure 1). In this case, there were less SPI-PEO interfacial areas as the response of increased protein concentration, explaining the lower dielectric constant. However, this phenomenon is not obvious in the sample with dialysis treated SPI. Thus, we may conclude that the dialysis can help with locking the structures of denatured SPI so that the decrease of the dielectric constant is relatively low.

Dielectric loss is the expression of the complex dielectric constant, which describes the loss of energy in a material through conduction under electric field [16]. As shown in Figure 4, second row, for all the three

denaturation conditions, the dielectric loss displayed fluctuations at low frequencies. As the SPI concentration increased, the fluctuation decreased. The main reason is fewer polar groups exposed on SPI particle surface caused by the protein aggregation at a high SPI concentration, being sensitive to the applied electric field. Compared to the other two protein denaturation conditions, the PEO composites with dialysis treated SPI presented the smallest amplitude of fluctuation, from low to high protein concentrations. Generally, the lower dielectric loss indicates the higher performance of the material for capacitor applications [16].

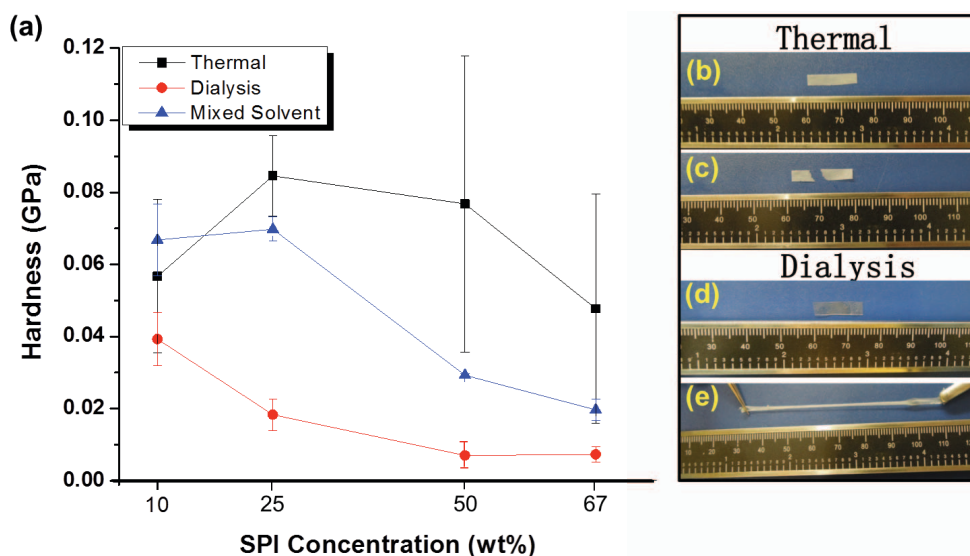


Figure 5: (a) Plot showing hardness values of PEO/SPI films as a function of SPI concentration for different denaturation conditions, (b-e) Photographs demonstrating the mechanical properties of PEO/SPI films (SPI concentration: 67%). (b) and (d) show the respective films before stretching, while (c) and (e) show the films after stretching.

3.4. Mechanical Properties

To demonstrate the differences in mechanical properties between different PEO/SPI composites, small pieces of the composite films were manually stretched, as shown in Figure 5. Brittleness is a characteristic property of both unmodified SPI and composites with high SPI concentrations [17]. In the current study, the PEO/SPI composites with both thermally denatured SPI and mixed solvent treated SPI show essentially a common brittle nature. However, the mechanical behavior of the composites with dialysis-treated SPI is markedly different. In Figure 5(a), average hardness results obtained from nanoindentation testing are presented. Hardness is a property that accounts for both elastic and plastic deformation of a material, which is more representative of the overall mechanical behaviors of the PEO/SPI composite systems in current study. [18] PEO/SPI composites with dialysis-treated SPI show significantly lower hardness values than samples with the other two treatment conditions for all SPI concentrations. At the highest SPI concentration, 67%, the hardness of the dialysis-treated SPI sample is only 15% of that of the thermally denatured SPI sample and 37% that of the mixed solvent treated sample. The behavior transition from brittle to soft as a result of dialysis treatment is confirmed when macroscopic pieces of the samples are stretched. Figure 5(b and c) exhibit an example of thermally denatured sample, while showing almost no elongation after stretch. In comparison, the sample containing dialysis-treated SPI displays ductile behavior. As shown in Figure 5(d and e), the dialyzed-SPI/PEO composite with the highest SPI concentration (67%) can elastically stretch to over five times its original length. Other investigations have shown that SPI has very strong interactions with PEO when these two components are effectively blended at the nanoscale [19]; it seems that this interaction results in molecular conformations that contribute to elastic behavior. The sample with thermally denatured SPI, on the other hand, not only has weaker PEO/SPI interactions but also contains larger particles (Figure 1 (a-d)) that may act as stress concentration sites, resulting in more brittle behavior.

4. CONCLUSIONS

According to the results obtained throughout this work, it is clear that the morphology and properties of the PEO/SPI composites are strongly affected by the SPI denaturation conditions, such as, thermal treatment, types of solvent, dialysis. By examining the

particle size distribution of SPI particles, the dialysis-treated SPI has the smallest particles resulting from the greatest number of intermolecular bonds broken, and therefore the denaturation is most effective compared to thermal and mixed solvent treated samples. Results of the light-scattering experiment are in strong agreement with this result, very little scattering occurs when the laser beam is passed through the dialysis denatured SPI solution, indicating a small particle size. Optical images of the composite films show that thermally denatured SPI has little effect on the PEO crystal structure, while the other two samples show significant changes in morphology with the addition of SPI, suggesting that the mixed-solvent and dialysis-treated SPI have a greater degree of unfolding and can therefore more effectively interact with PEO. Furthermore, changes in dielectric storage and loss modulus align closely with changes in morphology resulting from the different denaturation conditions; generally, as the particle size increases, the PEO-SPI interfacial area is reduced, resulting in a greater reduction in permittivity as the concentration of SPI is increased. Furthermore, the difference in denaturation degree is demonstrated in their mechanical properties: only the dialysis-treated samples show significant elastic behavior resulting from improved denaturation. Therefore, both the smaller particle size and unique mechanical behavior for the dialysis-treated samples show that this denaturation technique is the most effective of the three methods studied here.

This study confirms the critical importance of denaturation processes on the morphology and properties of protein-polymer composites, and provides a facile and valuable method for controlling the properties of the composites, which is very helpful for designing and fabricating soy-based polymeric materials.

REFERENCES

- [1] Carpiné D, Dagostin JLA, Bertan LC, Mafrá MR. Development and characterization of soy protein isolate emulsion-based edible films with added coconut oil for olive oil packaging: barrier, mechanical, and thermal properties. *Food Bioprocess Tech* 2015;8(8): 1811-1823. <http://dx.doi.org/10.1007/s11947-015-1538-4>
- [2] Jones A, Mandal A and Sharma S. Protein-based bioplastics and their antibacterial potential. *J Appl Polym Sci* 2015; 132(18): 41931. <http://dx.doi.org/10.1002/app.41931>
- [3] Guerrero P, Retegi A, Gabilondo N and de la Caba K. Mechanical and thermal properties of soy protein films processed by casting and compression. *J Food Eng* 2010; 100(1): 145-151. <http://dx.doi.org/10.1016/j.jfoodeng.2010.03.039>
- [4] Hughes GJ, Ryan DJ, Mukherjea R and Schasteen CS. Protein digestibility-corrected amino acid scores (PDCAAS)

- for soy protein isolates and concentrate: criteria for evaluation. *J Agr Food Chem* 2011; 59(23): 12707-12712. <http://dx.doi.org/10.1021/jf203220v>
- [5] Fakirov S and Bhattacharyya D. Handbook of engineering biopolymers: homopolymers, blends and composites. Hanser Gardner Publications. Inc Cincinnati 2007. <http://dx.doi.org/10.3139/9783446442504>
- [6] Salas C, Rojas O, Lucia L, Hubbe M and Genzer J. Adsorption of glycinin and β -conglycinin on silica and cellulose: Surface interactions as a function of denaturation, pH, and electrolytes. *Biomacromolecules* 2012; 13(2): 387-396. <http://dx.doi.org/10.1021/bm2014153>
- [7] Goli KK, Rojas OJ, OzçamAE and GenzerJ. Generation of functional coatings on hydrophobic surfaces through deposition of denatured proteins followed by grafting from polymerization. *Biomacromolecules* 2012; 13(5): 1371-1382. <http://dx.doi.org/10.1021/bm300075u>
- [8] Gennadios A, Brandenburg AH, Weller CL and Testin RF. Effect of pH on properties of wheat gluten and soy protein isolate films. *J Agr Food Chem* 1993; 41(11): 1835-18390. <http://dx.doi.org/10.1021/jf00035a006>
- [9] Fukushima D. Denaturation of soybean proteins by organic solvents. *Cereal Chem* 1969; 46: 156-163.
- [10] Myers J, Pace CN and Scholtz JM. Denaturant m values and heat capacity changes: relation to changes in accessible surface areas of protein unfolding. *Protein Sci* 1995; 4(10): 2138-2148. <http://dx.doi.org/10.1002/pro.5560041020>
- [11] Huang W and Sun X. Adhesive properties of soy proteins modified by urea and guanidine hydrochloride. *J Am Oil Chem Soc* 2000; 77(1): 101-104. <http://dx.doi.org/10.1007/s11746-000-0016-6>
- [12] Huang W and Sun X. Adhesive properties of soy proteins modified by sodium dodecyl sulfate and sodium dodecylbenzene sulfonate. *J Am Oil Chem Soc* 2000; 77(7): 705-708. <http://dx.doi.org/10.1007/s11746-000-0113-6>
- [13] Rhim JW, Gennadios A, Handa A, Weller CL and Hanna MA. Solubility, tensile, and color properties of modified soy protein isolate films. *J Agr Food Chem* 2000; 48(10): 4937-4941. <http://dx.doi.org/10.1021/jf0005418>
- [14] Wang J-W, Shen Q-D, Bao H-M, Yang C-Z and Zhang QM. Microstructure and dielectric properties of P(VDF-TrFE-CFE) with partially grafted copper phthalocyanineoligomer. *Macromolecules* 2005; 38(6): 2247-2252. <http://dx.doi.org/10.1021/ma047890d>
- [15] Li JY. Exchange coupling in P(VDF-TrFE) copolymer based all-organic composites with giant electrostriction. *Phys Rev Lett* 2003; 90(21): 217601. <http://dx.doi.org/10.1103/PhysRevLett.90.217601>
- [16] Nalwa HS. Handbook of low and high dielectric constant materials and their applications. Academic Press, San Diego 1999.
- [17] Zhang M, Song F, Wang X-L and Wang Y-Z. Development of soy protein isolate/waterborne polyurethane blend films with improved properties. *Colloid Surface B* 2012; 100: 16-21. <http://dx.doi.org/10.1016/j.colsurfb.2012.05.031>
- [18] Oyen M. Nanoindentation hardness of mineralized tissues. *J Biomech* 2006; 39(14): 2699-2702. <http://dx.doi.org/10.1016/j.jbiomech.2005.09.011>
- [19] Xu X, Jiang L, Zhou Z, Wu X and Wang Y. Preparation and properties of electrospun soy protein isolate/polyethylene oxide nanofiber membranes. *ACS Appl Mater Interfaces* 2012; 4(8): 4331-4337. <http://dx.doi.org/10.1021/am300991e>

Received on 26-10-2015

Accepted on 05-11-2015

Published on 31-12-2015

DOI: <http://dx.doi.org/10.12974/2311-8717.2015.03.02.1>

© 2015 Wei-Hong Zhong; Licensee Savvy Science Publisher.

This is an open access article licensed under the terms of the Creative Commons Attribution Non-Commercial License (<http://creativecommons.org/licenses/by-nc/3.0/>) which permits unrestricted, non-commercial use, distribution and reproduction in any medium, provided the work is properly cited.